IEEE Photonics Journal
An IEEE Photonics Society Publication

Open Access

High Bandwidth Freestanding Semipolar (11–22) InGaN/GaN Light-Emitting Diodes

Volume 8, Number 5, October 2016

Zhiheng Quan
Duc V. Dinh
Silvino Presa
Brendan Roycroft
Ann Foley
Mahbub Akhter
Donagh O'Mahony
Pleun P. Maaskant
Marian Caliebe
Ferdinand Scholz
Peter J. Parbrook
Brian Corbett

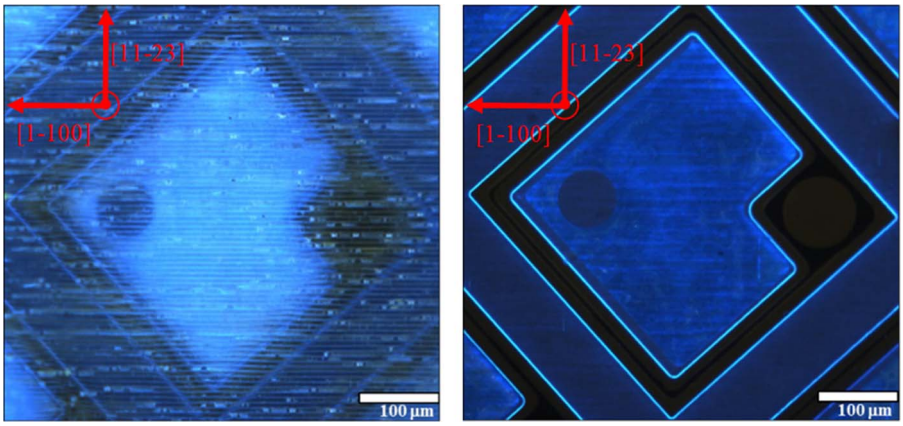

DOI: 10.1109/JPHOT.2016.2596245
1943-0655

IEEE photonics SOCIETY

IEEE

High Bandwidth Freestanding Semipolar (11–22) InGaN/GaN Light-Emitting Diodes

Zhiheng Quan,[1,2] Duc V. Dinh,[1] Silvino Presa,[1,2] Brendan Roycroft,[1] Ann Foley,[1] Mahbub Akhter,[1] Donagh O'Mahony,[1] Pleun P. Maaskant,[1] Marian Caliebe,[3] Ferdinand Scholz,[3] Peter J. Parbrook,[1,2] and Brian Corbett[1]

[1]Tyndall National Institute, University College Cork, Cork T12 R5CP, Ireland
[2]School of Engineering, University College Cork, Cork T12 YN60, Ireland
[3]Institute of Optoelectronics, Ulm University, 89081 Ulm, Germany

DOI: 10.1109/JPHOT.2016.2596245

Manuscript received June 24, 2016; revised July 21, 2016; accepted July 25, 2016. Date of publication August 26, 2016; date of current version September 22, 2016. This work was supported in part by the European Union Seventh Framework Programme ALIGHT Project under Agreement FP7-280587 and in part by the Science Foundation Ireland through the Irish Photonic Integration Centre Program under Grant 12/RC/2276. Corresponding author: Z. Quan (e-mail: zhiheng.quan@tyndall.ie).

Abstract: Freestanding semipolar (11–22) indium gallium nitride (InGaN) multiple-quantum-well light-emitting diodes (LEDs) emitting at 445 nm have been realized by the use of laser lift-off (LLO) of the LEDs from a 50-μm-thick GaN layer grown on a patterned (10–12) *r*-plane sapphire substrate (PSS). The GaN grooves originating from the growth on PSS were removed by chemical mechanical polishing. The 300 μm × 300 μm LEDs showed a turn-on voltage of 3.6 V and an output power through the smooth substrate of 0.87 mW at 20 mA. The electroluminescence spectrum of LEDs before and after LLO showed a stronger emission intensity along the $[11\text{–}23]_{InGaN/GaN}$ direction. The polarization anisotropy is independent of the GaN grooves, with a measured value of 0.14. The bandwidth of the LEDs is in excess of 150 MHz at 20 mA, and back-to-back transmission of 300 Mbps is demonstrated, making these devices suitable for visible light communication (VLC) applications.

Index Terms: Light-emitting diodes (LEDs), optoelectronic materials, semipolar gallium nitride (GaN), laser lift-off (LLO), metal organic vapor phase epitaxy (MOVPE).

1. Introduction

Wurtzite indium gallium nitride (InGaN) based light-emitting diodes (LEDs) have demonstrated exceptional efficiency and output powers in the visible spectral range. The LEDs are attractive light sources for use in visible light communication (VLC), which is a promising technology using energy-efficient light source illumination with data encoded to achieve optical data transmission that has significant potential to supplement existing radio-frequency (RF) based wireless communications. It has attracted much interest recently, as it can provide new large data transmission capacity in license-free and can, in principle, be integrated into preexisting lightning infrastructure [1]–[4]. Commercially available InGaN-based LEDs are grown on the *c*-plane (0001) oriented surface, which have strong built-in piezoelectric fields. The piezoelectric polarization fields at the InGaN/GaN interface tilt the energy band of the quantum-well (QW) based active region. This induces a quantum-confined stark effect (QCSE), lowering the electron-hole

overlap and device efficiency [5], as well as inducing wavelength shift with current. A reduction in the QCSE will increase the overlap of the electron and hole wavefunctions and, therefore, increase the radiative recombination rate. Hence, it is desirable to produce InGaN/GaN QW LEDs with a suppression of the internal fields [5]–[12] for high bandwidth devices [1]–[4].

The fields can be reduced by growing LEDs on semipolar and non-polar oriented surfaces of the crystal [13], [14]. The semipolar (11–22) surface is of special interest because high-efficiency green and yellow LEDs have been previously reported [15]–[18] with best results for devices grown on bulk (11–22) GaN substrates [15]. Such substrates are very expensive and small in size and thus not suitable for mass-production. Thus, it is preferable to grow LEDs on a low-cost sapphire substrate. However, (11–22) GaN films grown on non-patterned (10-10) *m*-plane sapphire substrates normally contain a high density of extended defects such as basal-plane stacking faults, prismatic stacking faults and partial dislocations [19]. In order to reduce such defects, several approaches have been proposed in recent years [20]–[22]. Here, we grow the LEDs on a 50 μm-thick GaN template which was grown on a patterned (10–12) *r*-plane sapphire substrate (PSS) using a growth process which has been scaled to 100 mm diameter wafers [23].

In this paper, we demonstrate a laser-lift-off (LLO) technique for obtaining freestanding semipolar (11–22) InGaN/GaN multi-quantum-well (MQW) LEDs operating at $\sim$445 nm. We found that Ni/Ag/Ni acted as a quasi-ohmic p-contact metal with good reflection improving the light output through the substrate. We characterized the electrical and optical properties (light output power, electroluminescence (EL) spectra, and optical polarization). The output power of the LEDs was enhanced after LLO. A stable light emission with an anisotropic emission pattern was observed. The polarization ratio was calculated for the LEDs after LLO and after chemical mechanical polishing (CMP). The electro-optical bandwidth of the LEDs was 166 MHz at 20 mA biased current and demonstrate a transmission data rate of 300 Megabits per second (Mbps), which can be suitable for VLC.

2. Experiment

The LED structure was grown on the (11–22) oriented surface of a GaN template on a PSS. The template was prepared in two stages [24]–[26]. Firstly, a 6 μm-thick GaN layer was grown by metal organic vapor phase epitaxy (MOVPE) on a PSS which was patterned with 1 μm deep grooves on a 6 μm pitch oriented along the [11-20]. *a*-direction of sapphire ([10-10] *m*-direction of GaN). A SiN interlayer was used to reduce the defect density and a very low basal-plane stacking fault density was obtained. Subsequently, a $\sim$50 μm-thick GaN layer was grown by hydride vapor phase epitaxy (HVPE) [24]–[26]. The wafer was diced into 2 cm $\times$ 2 cm pieces, and CMP was used to smoothen the HVPE-grown template surface. The LED structure was grown on this template and consisted of 1.5 μm-thick Si-doped n-type GaN, 120 nm-thick n-$In_{0.01}Ga_{0.99}N$, five periods of InGaN/GaN (2.5 nm/6.5 nm) QW active region, 120 nm-thick Mg-doped p-type GaN, and 15 nm heavily doped p-type GaN contact layer. Details of the LED growth conditions and CMP process are reported elsewhere [18]. A particular issue with semipolar GaN planes is the difficulty in obtaining high p-type doping with Mg. A $\times$ 4 higher Mg flux is required to obtain the same incorporation in the (11–22) crystal as compared with c-plane [12], [27]. Secondly, the acceptors show higher compensation due to unintentional oxygen impurity and, as a result, it is difficult to obtain a high free hole concentration resulting in non-ohmic p-contacts. We compared Ni/Ag/Ni (1 nm/100 nm/2 nm thick) and Pd (40 nm thick) as p-type contacts using the circular transfer length method (cTLM). The Ni/Ag/Ni formed a quasi-ohmic contact after rapid thermal annealing (RTA) at 500 °C under oxygen for 60 s. The Ag interlayer also provides high reflectivity enhancing the light emission through the substrate. However, the as-deposited Pd contacts show non-ohmic properties as shown in Fig. 1.

Freestanding (1 cm $\times$ 1 cm size) sample containing LEDs (300 μm $\times$ 300 μm) were fabricated using photolithography and dry etching techniques. The fabrication sequence is illustrated in Fig. 2. The p-type contact metal of Ni (1 nm)/Ag (100 nm)/Ni (2 nm) was annealed using

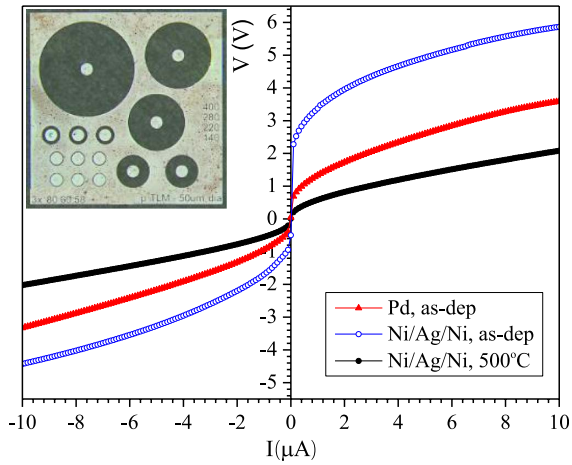

Fig. 1. Current–voltage *I–V* characteristics of a 50-μm diameter disk contact with a gap of 280 μm on (inset) cTLM pattern of Pd (40 nm) as-deposited and Ni (1 nm)/Ag (100 nm)/Ni (2 nm) before and after anneal at 500 °C.

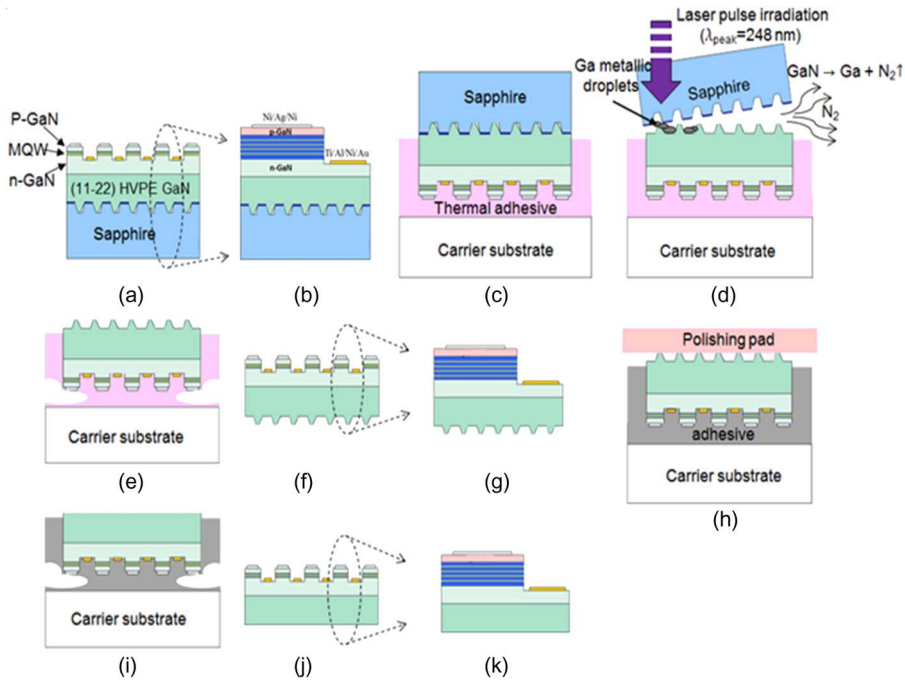

Fig. 2. Schematic of the fabrication process for obtaining freestanding semipolar (11–22) LEDs by the use of LLO and CMP techniques. (a) Fabrication of LEDs on patterned sapphire substrate (PSS). (b) 300 μm $\times$ 300 μm mesa LED chip on PSS. (c) Wafer flip bonded with thermal adhesive on glass carrier substrate. (d) LLO of LED wafer and removal of the PSS. (e) Debond sample and dissolve the adhesive layer. (f) Freestanding LEDs with grooves (LLO-LED). (g) LLO-LED chip. (h) Flip bond and CMP. (i) Debond and dissolve adhesive layer. (j) Freestanding LEDs without grooves (CMP-LED). (k) CMP-LED chip.

RTA. Mesas were etched to a depth of 1 μm exposing the n-type GaN by using inductively coupled plasma etching. The LED chip was then bonded with thermo-adhesive (Crystal-bond 509 clear wax) onto a glass slide as a temporary substrate. The sapphire substrate was removed by laser-induced delamination of the GaN stripes attached to the sapphire interface. Single-shot

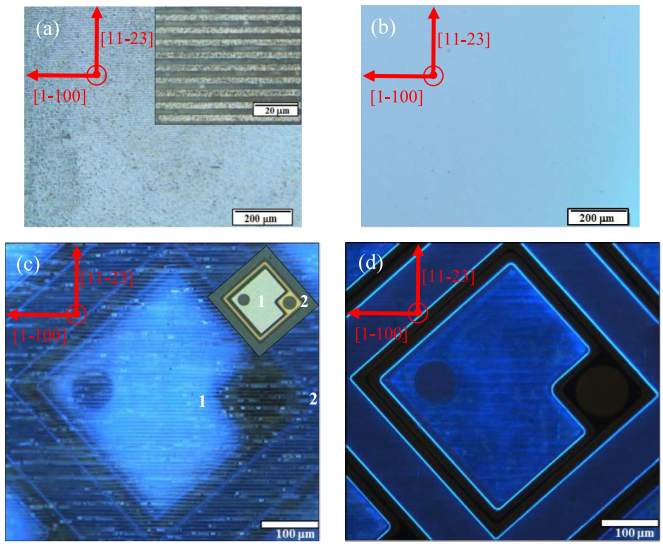

Fig. 3. Optical microscope images of the back surface (a) after LLO (Inset: GaN grooves in plan view) and (b) after CMP. FM images ($560 \times 560\ \mu m^2$) of the backside of the LEDs (c) after LLO (Inset: Top view image of the fabricated LEDs, where area 1 is the p-metal and area 2 is the n-metal) and (d) after CMP.

laser pulses (irradiation density of 500 mJ/cm^2) were scanned across the sample using a KrF excimer laser system (ATLEX-300-SI) to remove the wafer from the substrate without damage. The $\sim$50 μm-thick sample was de-bonded by dissolving the adhesive in acetone. The devices were characterized, and no detrimental effect on the light optical power was found due to the LLO process. Subsequently the sample was bonded with thermal adhesive (i.e. black wax) on a Si substrate and the grooves on the back surface of the wafer were removed by CMP. Finally, freestanding LEDs were obtained by dissolving the black wax.

The Nomarski images of the morphology on the back surface of the LED after LLO (LLO-LED) and LED after CMP (CMP-LED) are shown in Fig. 3(a) and (b), respectively. The LLO-LED back surface has structured grooves (approximately 3 μm wide and 2 μm high) due to the GaN stripes associated with the growth initiation on the PSS which can be seen in inset image of Fig. 3(a). In contrast, the morphology of the CMP-LEDs is very smooth as shown in Fig. 3(b). A fluorescence microscope (FM) image obtained with the 405 nm line of a mercury lamp was used to investigate the uniformity of the QW luminescence through the back surface of the LED samples. The emission was detected by a color camera, thus producing a real-color representation of the QW emission. Fig. 3(c) and (d) show the FM images of the QWs (peak emission wavelength $\sim$445 nm) after LLO and after CMP of the grooves respectively. The very uniform luminescence of the LEDs can be observed from both images on the active region. It is seen that the p-contact region is brighter than the region without the p-metal due to the reflection of Ag interlayer. Moreover, the intensity in Fig. 3(c) is higher than Fig. 3(d), which is due to the light scattering caused by the GaN grooves. Fig. 3(c) and (d) show bright emission from the mesa edges which may indicate stronger light emission in the plane of the QWs but is also due to light scattering at the mesa edges.

3. Results and Discussion

EL measurements were taken from the 300 μm $\times$ 300 μm LEDs at each stage in the process with the light output collected from the backside of the devices with numerical apertures (NA) of 0.5 and 1.0 into a calibrated Si photodetector. The spectra of the LEDs were recorded with an Ocean Optics spectrometer with a silica optical fiber coupled to the backside of the LEDs. The light output power (L–I) and voltage (V–I) with current of the non-LLO LED, LLO-LED,

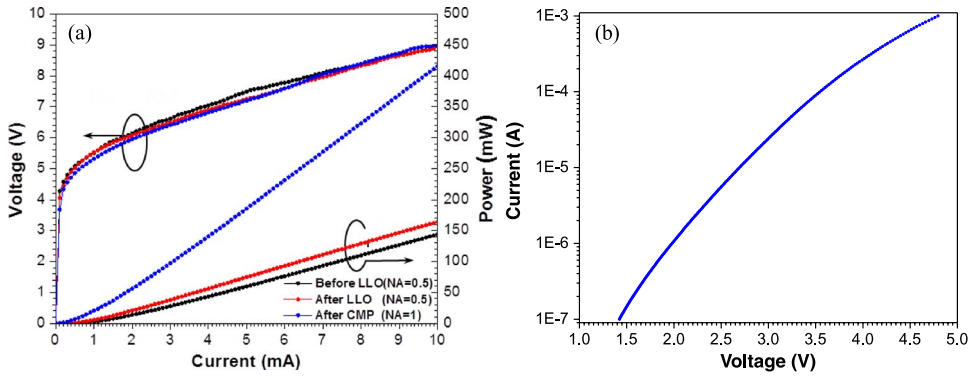

Fig. 4. (a) *L–I* and *V–I* characteristics of the LEDs before and after LLO measured into a detector with a numerical aperture NA of 0.5 and after CMP (measured with NA of 1). (b) Semilog IV of a freestanding (11–22) LED GaN LED after CMP.

and CMP-LED are shown in Fig. 4(a). The *V–I* characteristics for the CMP- and non-CMP-LEDs are similar with a threshold voltage of ∼3.6 V. The series resistance is found to be 368 Ω. The light output power of the LEDs after LLO is enhanced by 14% at 10 mA compared with the LEDs before LLO, which is due to the light scattering caused by the GaN groove features on the back surface. The light output power of CMP-LED is lower than the LLO-LED with grooves when measured in our standard configuration (i.e. NA = 0.5). However, to compare with results reported from other groups, the output power of the CMP-LED was also measured with NA of 1. The measured output power of the CMP-LEDs with an NA of 1, i.e. directly on the photodetector is 870 μW at 20 mA ($J = 22$ A/cm^2), which is comparable to other blue semipolar (11–22) InGaN LEDs grown on sapphire substrates [28]–[30]. For example, an output power of ∼1.8 mW has been obtained for a packaged (11–22) LED grown on GaN bulk substrate with the chip size of 320 μm × 320 μm ($J = 20$ A/cm^2, $I = 20$ mA) emitting at 420 nm [28], ∼0.38 mW has been obtained for a 280 μm-diameter unpackaged (11–22) LED grown on GaN/sapphire template ($J = 33$ A/cm^2, $I = 20$ mA) emitting at 422 nm [29], and ∼1.0 mW has been obtained for a unpackaged (11–22) LED grown on GaN/sapphire template grown on patterned sapphire substrate emitting at 440 nm with the chip size 1100 μm × 600 μm ($J = 3$ A/cm^2, $I = 20$ mA) [30]. For the LEDs studied here, one can be expected that the output power will significantly increase with fully packaged devices through controlled surface roughening and epoxy encapsulation. Fig. 4(b) shows the log *I–V* characteristics of the freestanding semipolar LEDs for currents from 100 nA to 1 mA indicating that the LEDs have no shunt paths but a small non-radiative leakage current, which delays the light emission until voltages larger than 3 V.

Fig. 5(a) shows the normalized EL spectra at currents up to 10 mA ($J = 11$ A/cm^2) of the LEDs after LLO. With increasing drive current, the EL peak emission at ∼445 nm is stable with a wavelength shift of about 1.1 nm for a current density change to 11 A/cm^2.

An optical polarization anisotropy was observed in the EL from the LEDs both before and after LLO with the stronger emission intensity along the [11-23] inclined *c′*-direction, as shown in Fig. 6. An elongated light emission pattern is formed due to the scattering from the grooves. The EL emission intensity as a function of polarization angle for the freestanding (11–22) LEDs after LLO and after CMP, both at 2 mA driven current, was measured. When the polarizer is placed along the elongated direction of the GaN grooves i.e. the [1–100] *m*-axis (i.e. 0° and 180°), the EL emission intensity is maximized. The minimum of EL emission intensity occurs for the polarizer set along the [11-23] *c′*-axis (i.e., 90° and 270 °C). The polarization ratio is independent of the GaN grooves, both the LLO- and CMP-LEDs show a polarization ratio $\rho_{\text{polar}} = (I_{\max} - I_{\min})/(I_{\max} + I_{\min})$ of 0.14. With the grooves present the light emission shows a larger light broadening along *m*- and *c′*-directions. After CMP, a more uniform spot-like emission is obtained indicating the role of the grooves on the emission pattern.

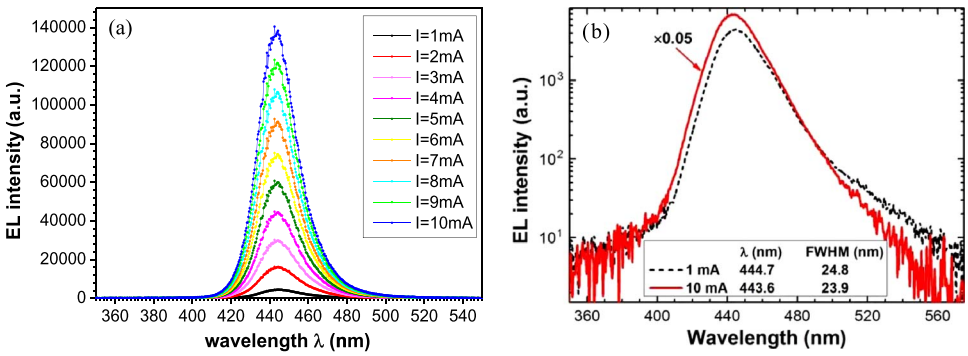

Fig. 5. (a) EL spectra of the freestanding semipolar LED as a function of current up to 10 mA (11 A/cm^2). (b) Normalized EL spectra of the freestanding semipolar LEDs at 1 and 10 mA.

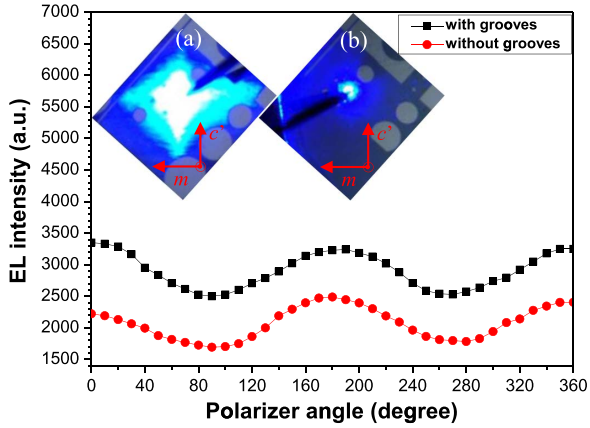

Fig. 6. EL intensity with polarization angle for the freestanding semipolar (11–22) InGaN/GaN LED (LLO-LED and CMP-LED). Inset: (a) Anisotropic light emission profile after LLO and (b) more uniform spot like emission after CMP.

Due to the reduced piezoelectric field an increased overlap of the electron and hole wave functions is expected resulting in a faster radiative lifetime. The LEDs can, therefore, be expected to have a high bandwidth, even though the epitaxial structure and the device mesa geometry were not optimized for the bandwidth. The small-signal frequency response of both freestanding semipolar LEDs along with a reference commercial *c*-plane GaN LED emitting at 466 nm grown on double polished sapphire substrate with same mesa size (light output power at 20 mA is 2.45 mW) was measured on-chip as a function of current using a microwave probe (DC to 3.5 GHz). A sinusoidal signal with low RF power from a vector network analyzer (Agilent 8753ES) was applied on top of a DC bias using a bias tee (Mini-Circuits 15542 ZFBT-6GW-FT 9628). The light output from the LED was collected with a lens of 2 cm diameter and focused on a high bandwidth (1.4 GHz) silicon PIN photodiode with integrated transimpedance amplifier (TIA) photoreceiver (HAS-X-S-1G4-SI) and the frequency response was recorded by the vector network analyzer at different bias currents. The measured -3 dB bandwidths as a function of current are shown in Fig. 7(a) and compared with the reported bandwidth of high-speed LEDs on (0001) and semipolar (11–22) planes [31]–[34]. For the (11–22) LEDs studied here, when the device was biased at 20 mA, a modulation frequency of 166 MHz was obtained, while the reference *c*-plane LED has the lowest bandwidth of 38 MHz. The bandwidth of *c*-plane LEDs in smaller dimension are compared with semipolar (11–22) LED in larger dimension to show a dependence on the driving current. The 300 μm $\times$ 300 μm (11–22) LEDs emitting at 500 nm and 450 nm grown on PSS show the bandwidth at 72 MHz and 100 MHz, respectively [34]. The 75-μm diameter *c*-plane LEDs emitting at 441 nm and

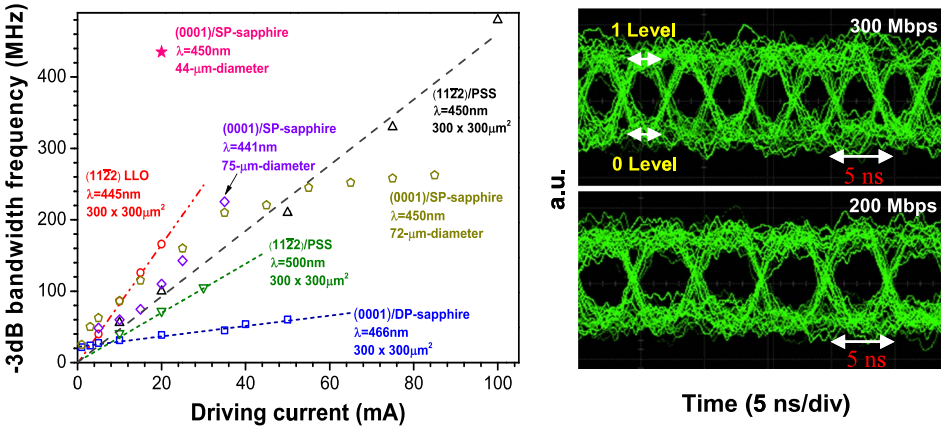

Fig. 7. (a) Small signal bandwidth at −3 dB of the (○) 300 μm × 300 μm freestanding (11–22) LED and the (□) 300 μm × 300 μm *c*-plane GaN LED, as compared with the high-speed GaN-based LEDs reported in the literature. (△) Reference [34] 300 μm × 300 μm (11–22) blue LED. (▽) Reference [34] 300 μm × 300 μm (11–22) green LED. (⬠) Reference [31] 72-μm diameter *c*-plane GaN LED. (★) Reference [32] 44-μm diameter *c*-plane GaN LED. (◇) Reference [33] 75-μm diameter *c*-plane GaN LED. (b) Eye diagrams at 300 Mbps and 200 Mbps of the freestanding (11–22) LED.

72-μm diameter emitting at 450 nm grown on single polished sapphire substrate show the bandwidth 110 MHz ($J = 450$ A/cm^2, $I = 20$ mA) and 150 MHz ($J = 490$ A/cm^2, $I = 20$ mA), respectively [31], [32]. The smaller dimensional LED of 44-μm diameter *c*-plane LED grown on single polished sapphire ($J = 1.3$ kA/cm^2, $I = 20$ mA) emitting at 450 nm shows a higher bandwidth, which is 435 MHz [33].

The large signal properties of the freestanding semipolar LEDs were measured. To determine the transmission data rate of the freestanding semipolar LED, a 2^7-1 non-return-to-zero (NRZ) pseudo-random bit sequence (PRBS)-7 from a pattern signal generator (Anritsu MP1632A) was added at each DC bias and the eye diagrams were collected by a digital oscilloscope (Agilent Infinilum DSO80804A). When a 2 V peak-to-peak amplitude is applied as the large signal modulation with the LEDs biased at 20 mA, the transmitted data rate for the open eye diagram can be up to 300 Mbps (see Fig. 7).

4. Conclusion

We have demonstrated a fabrication process to realize freestanding semipolar (11–22) InGaN/GaN MQW LEDs on a HVPE GaN template by the use of LLO and CMP. No detrimental effect in the light optical power was observed due to the LLO process. The NiAgNi p-metal provided a better light extraction and low contact resistance for substrate emitting LEDs. The emission properties were stable. The output power of the freestanding semipolar GaN LEDs (after CMP) was 0.87 mW at 20 mA without any extraction features or low index encapsulation. The polarization ratio was 0.14 and was independent of the GaN grooved features. The LEDs showed an electrical-to-optical bandwidth of 166 MHz at 20 mA and the signal transmission data rate of 300 Mbps, which is promising for VLC applications. It can be expected that smaller dimensional LEDs will have lower capacitance and the bandwidth will be higher.

References

[1] D. O'Brien, G. Parry, and P. Stavrinou, "Optical hotspots speed up wireless communication," *Nat. Photon.*, vol. 1, no. 5, pp. 245–247, May 2007.
[2] H. Elgala, G. Parry, and H. Haas, "Indoor optical wireless communication: Potential and state-of-the-art," *IEEE Commun. Mag.*, vol. 49, no. 9, pp. 56–62, Sep. 2011.

[3] S. Haruyama, "Advances in visible light communication technologies," in *Proc. IEEE Eur. Conf. Exhib. Opt. Commun., OSA*, Sep. 2012, pp. 1–3.
[4] I. Takai, T. Harada, M. Andoh, K. Yasutomi, K. Kagawa, and S. Kawahito, "Optical vehicle to vehicle communication system using LED transmitter and camera receiver," *IEEE Photon. J.*, vol. 6, no. 5, pp. 1–14, Oct. 2014.
[5] T. Wang, D. Nakagawa, J. Wang, T. Sugahara, and S. Sakai, "Photoluminescence investigation of InGaN/GaN single quantum well and multiple quantum wells," *Appl. Phys. Lett.*, vol. 73, no. 24, p. 3571, Oct. 1998.
[6] P. Waltereit *et al.*, "Nitride semiconductors free of electrostatic fields for efficient white light emitting diodes," *Nature*, vol. 406, no. 6798, pp. 865–868, Aug. 2000.
[7] M. C. Schmidt *et al.*, "Demonstration of nonpolar m-plane InGaN/GaN laser diodes," *Jpn. J. Appl. Phys.*, vol. 46, no. 2, pp. 8–11, Feb. 2007.
[8] Y. Zhao *et al.*, "Optimization of device structures for bright blue semipolar (1011) light emitting diodes via metalorganic chemical vapor deposition," *Jpn. J. Appl. Phys.*, vol. 49, no. 7R, Jul. 2010, Art. no. 070206.
[9] N. F. Gardner, J. C. Kim, J. J. Wierer, Y. C. Shen, and M. R. Krames, "Polarization anisotropy in the electroluminescence of m-plane InGaN-GaN multiple-quantum-well light emitting diodes," *Appl. Phys. Lett.*, vol. 86, no. 11, Jan. 2005, Art. no. 111101.
[10] F. Scholz, "Semipolar GaN grown on foreign substrates: A review," *Semicond. Sci. Technol.*, vol. 27, no. 2, Jan. 2012, Art. no. 024002.
[11] T. Wunderer *et al.*, "Three-dimensional GaN for semipolar light emitters," *Phys. Status Solidi B.*, vol. 248, no. 3, pp. 549–560, Mar. 2011.
[12] H. Sato *et al.*, "High power and high efficiency semipolar InGaN light emitting diodes," *J. Light Vis. Environ.*, vol. 32, no. 2, pp. 107–110, Feb. 2008.
[13] D. F. Feezell, J. S. Speck, S. P. DenBaars, and S. Nakamura, "Semipolar (20-2-1) InGaN/GaN light-emitting diodes for high-efficiency solid-state lighting," *J. Display Technol.*, vol. 9, no. 4, pp. 190–198, Apr. 2013.
[14] C. Wetzel *et al.*, "Light-emitting diode development on polar and non-polar substrates," *J. Cryst. Growth*, vol. 310, no. 17, pp. 3987–3991, Aug. 2008.
[15] H. Sato *et al.*, "Optical properties of yellow light-emitting diodes grown on semipolar (11-22) bulk GaN substrates," *Appl. Phys. Lett.*, vol. 92, no. 22, Jun. 2008, Art. no. 221110.
[16] S. H. Park *et al.*, "Polarization characteristics of semipolar (11–22) InGaN/GaN quantum well structures grown on relaxed InGaN buffer layers and comparison with experiment," *Opt. Exp.*, vol. 22, no. 12, pp. 14850–14858, Jun. 2014.
[17] N. Okada, K. Uchida, S. Miyoshi, and K. Tadatomo, "Green light-emitting diodes fabricated on semipolar (11–22) GaN on r-plane patterned sapphire substrate," *Phys. Status Solidi A.*, vol. 209, no. 3, pp. 469–472, Mar. 2012.
[18] D. V. Dinh *et al.*, "Semipolar (11–22) InGaN light emitting diodes grown on chemically-mechanically polished GaN templates," *Phys. Status Solidi A.*, vol. 212, no. 10, pp. 2196–2200, Jun. 2015.
[19] T. Wernicke, C. Netzel, M. Weyers, and M. Kneissl, "Semipolar GaN grown on m-plane sapphire using MOVPE," *Phys. Status Solidi C.*, vol. 5, no. 6, pp. 1815–1817, Apr. 2008.
[20] Q. Sun, B. Leung, C. D. Yerino, Y. Zhang, and J. Han, "Improving microstructural quality of semipolar (11–22) GaN on m-plane sapphire by a two-step growth process," *Appl. Phys. Lett.*, vol. 95, no. 23, Dec. 2009, Art. no. 231904.
[21] P. de Mierry, N. Kriouche, M. Nemoz, S. Chenot, and G. Nataf, "Semipolar GaN films on patterned *r*-plane sapphire obtained by wet chemical etching," *Appl. Phys. Lett.*, vol. 96, no. 23, Jun. 2010, Art. no. 231918.
[22] N. Kriouche, P. Vennegues, M. Nemoz, G. Nataf, and P. de Mierry, "Stacking faults blocking process in (11–22) semipolar GaN growth on sapphire using asymmetric lateral epitaxy," *J. Cryst. Growth*, vol. 312, no. 19, pp. 2625–2630, Sep. 2010.
[23] F. Brunner *et al.*, "Semi-polar (11–22)-GaN templates grown on 100 mm trench-patterned r-plane sapphire," *Phys. Status Solidi B.*, vol. 252, no. 5, pp. 1189–1194, May 2015.
[24] F. Scholz *et al.*, "Semipolar GaN-based heterostructures on foreign substrates," *Phys. Status Solidi B.*, vol. 253, no. 1, pp. 13–22, Jan. 2016.
[25] M. Caliebe, T. Meisch, M. Madel, and F. Scholz, "Effects of miscut of prestructured sapphire substrates and MOVPE growth conditions on (11–22) oriented GaN," *J. Cryst. Growth*, vol. 414, pp. 100–104, Mar. 2015.
[26] M. Caliebe *et al.*, "Growth and coalescence studies of (11–22) oriented GaN on pre-structured sapphire substrates using marker layers," *Phys. Status Solidi B*, vol. 253, no. 1, pp. 46–53, Aug. 2015.
[27] T. Meisch *et al.*, "Doping behavior of (11–22) GaN grown on patterned sapphire substrates," *Phys. Status Solidi B.*, vol. 253, no. 1, pp. 164–168, Jan. 2016.
[28] M. Funato *et al.*, "Blue, green, and amber InGaN/GaN light-emitting diodes on semipolar (11–22) GaN bulk substrates," *Jpn. J. Appl. Phys.*, vol. 45, no. 2, pp. 24–28, Jun. 2006.
[29] S. Y. Bae *et al.*, "Electroluminescence enhancement of semipolar GaN light-emitting diodes grown on miscut m-plane sapphire substrates," *Curr. Appl. Phys.*, vol. 11, no. 3, pp. 954–958, May 2011.
[30] D. S. Kim, S. Lee, D. Y. Kim, S. K. Sharma, S. M. Hwang, and Y. G. Seo, "Highly stable blue-emission in semipolar (11–22) InGaN/GaN multi-quantum well light-emitting diode," *Appl. Phys. Lett.*, vol. 103, no. 2, Jul. 2013, Art. no. 021111.
[31] J. Mckendry *et al.*, "High speed visible light communications using individual pixels in a micro light-emitting diode array," *IEEE Photon. Technol. Lett.*, vol. 22, no. 18, pp. 1346–1348. Jul. 2010.
[32] J. Mckendry *et al.*, "Visible-light communications using a CMOS-controlled micro-light-emitting-diode array," *J. Lightw. Technol.*, vol. 31, no. 8, pp. 1211–1216, Jan. 2012.
[33] C. L. Liao, Y. F. Chang, C. L. Ho, and M. C. Wu, "High speed GaN-based blue light emitting diodes with gallium-doped ZnO current spreading layer," *IEEE Electron Device Lett.*, vol. 34, no. 5, pp. 611–613, May 2013.
[34] B. Corbett *et al.*, "Development of semipolar (11–22) LEDs on GaN templates," in *Proc. 20th SPIE Conf. Light-Emitting Diodes: Mater., Devices, Appl. Solid State Light.*, vol. 97681G, Mar. 2016, pp. 1–9.